



Magnetic field at Ce impurities in La sites of $\text{La}_{0.5}\text{Ba}_{0.5}\text{MnO}_3$ double perovskites

Cite as: AIP Advances **9**, 035245 (2019); <https://doi.org/10.1063/1.5080094>

Submitted: 05 November 2018 . Accepted: 12 February 2019 . Published Online: 22 March 2019

B. Bosch-Santos , N. M. Nascimento, M. Saiki, E. L. Correa, T. S. N. Sales, L. F. D. Pereira, G. A. Cabrera-Pasca, R. N. Saxena , J. Schell, and A. W. Carbonari 

COLLECTIONS

Paper published as part of the special topic on [2019 Joint MMM-Intermag Conference](#), [Chemical Physics](#), [Energy, Fluids and Plasmas](#), [Materials Science](#) and [Mathematical Physics](#)



View Online



Export Citation



CrossMark

ARTICLES YOU MAY BE INTERESTED IN

[A hyperfine look at titanium dioxide](#)

AIP Advances **9**, 085208 (2019); <https://doi.org/10.1063/1.5097459>

[Perturbed angular correlations at ISOLDE: A 40 years young technique](#)

AIP Advances **7**, 105017 (2017); <https://doi.org/10.1063/1.4994249>

[Anomalous behavior of the magnetic hyperfine field at \$^{140}\text{Ce}\$ impurities at La sites in \$\text{LaMnSi}_2\$](#)

AIP Advances **8**, 055702 (2018); <https://doi.org/10.1063/1.5006897>

AIP Advances Nanoscience Collection

READ NOW!

Magnetic field at Ce impurities in La sites of $\text{La}_{0.5}\text{Ba}_{0.5}\text{MnO}_3$ double perovskites

Cite as: AIP Advances 9, 035245 (2019); doi: 10.1063/1.5080094
Presented: 18 January 2019 • Submitted: 5 November 2018 •
Accepted: 12 February 2019 • Published Online: 22 March 2019



B. Bosch-Santos,^{1,a)}  N. M. Nascimento,¹ M. Saiki,¹ E. L. Correa,¹ T. S. N. Sales,¹ L. F. D. Pereira,¹
G. A. Cabrera-Pasca,² R. N. Saxena,¹  J. Schell,^{3,4} and A. W. Carbonari¹ 

AFFILIATIONS

¹Instituto de Pesquisas Energéticas e Nucleares, University of São Paulo, 05508-000 São Paulo, Brazil

²Faculdade de Ciências Exatas e Tecnologia, Universidade Federal do Pará, 68440-000 Abaetetuba, PA, Brazil

³Institute for Materials Science and Center for Nanointegration Duisburg-Essen (CENIDE), University of Duisburg-Essen, 45141 Essen, Germany

⁴European Organization for Nuclear Research (CERN), CH-1211 Geneva, Switzerland

Note: This paper was presented at the 2019 Joint MMM-Intermag Conference.

^{a)}Corresponding author: brianna@usp.br

ABSTRACT

Due to its rich variety of electromagnetic properties, such as a colossal magnetoresistance, charge and orbital ordering, and metal-insulator transition, the magnetic behavior in $\text{La}_{0.5}\text{Ba}_{0.5}\text{MnO}_3$ double perovskite compounds has been investigated by several techniques, however more experimental data, especially from atomic resolution techniques, are still necessary to understand such complex behavior. In this paper, we have used a nuclear and short-range technique, the Perturbed Angular Correlation (PAC) spectroscopy, to investigate the magnetic hyperfine interaction at the ^{140}Ce and ^{111}Cd probe nuclei as impurities occupying La sites. This double perovskite samples were synthesized by Sol-Gel route. The crystal structure was determined by X-ray diffraction and the analyses showed that this method produced perovskite oxides with cubic structure in $Pm-3m$ space group and the homogeneity was determined by Transmission Electron Microscopy (TEM). The local properties investigated by PAC spectroscopy revealed a ferromagnetic transition temperature above 300 K and a pure antiferromagnetic interaction below 100 K. Moreover, it also indicates an anomalous behavior of the temperature dependence of magnetic hyperfine field at La sites measured with ^{140}Ce probe nuclei, which can be ascribed to the contribution of $4f$ band of Ce to Magnetic Hyperfine Field (B_{hf}) at low temperatures due to the increase in its localized character.

© 2019 Author(s). All article content, except where otherwise noted, is licensed under a Creative Commons Attribution (CC BY) license (<http://creativecommons.org/licenses/by/4.0/>). <https://doi.org/10.1063/1.5080094>

I. INTRODUCTION

The series of cobaltite and manganite double oxide perovskites present a large variety of physical behaviors. Magnetic, electronic and lattice interactions lead to cooperative phenomena like superconductivity, electron transport, colossal magnetoresistance (associated to manganites) and lower magneto-resistance (associated to cobaltites) are topics of advanced research in Physics and Materials Science. These materials having a magnetoresistance are a focus of interest due to their applications in improving magnetic data storage. The family of double perovskites $\text{LaBaTM}_{2-\delta}\text{O}_{6-\delta}$ (TM = Mn, Co) showing multi-magnetic transitions, such as paramagnetic to ferromagnetic and to antiferromagnetic,^{1,2} have been investigated

intensively in the last decades because these compounds also present a rich variety of interesting properties, more specifically, colossal magnetoresistance, charge and orbital ordering, and metal-insulator transition.^{3,4} Due to these properties, these compounds are good candidates for important technological applications such as oxidation catalysts, gas sensors and electron conduction devices.¹ Specifically, $\text{LaBaTM}_2\text{O}_6$ compounds crystallize in a tetragonal structure with space group $P4/mmm$, however, these materials can present a disordered phase crystallizing in $\text{La}_{0.5}\text{Ba}_{0.5}\text{TMO}_3$ compounds, with oxygen deficiency and cubic structure ($Pm-3m$ space group) due to the ordering of R^{3+} and Ba^{2+} ions changing the phase diagram.⁵

In specific $\text{LaBaMn}_2\text{O}_6$ has been previously reported to show a ferromagnetic transition below 330 K and an antiferromagnetic

state below 150 K, but for the disorder phase, $\text{La}_{0.5}\text{Ba}_{0.5}\text{MnO}_3$, the ferromagnetic transition is around 280 K and the antiferromagnetic transition is below 200 K.⁵⁻⁷

Small microparticles of $\text{La}_{0.5}\text{Ba}_{0.5}\text{MnO}_3$ double perovskites are here investigated within an atomic resolution to understand their magnetic properties and to observe the Mn-O-Mn exchange interactions by a hyperfine interactions technique, the perturbed angular correlation (PAC) spectroscopy with ^{140}Ce and $^{111\text{m}}\text{Cd}$ as probe nuclei. Because ^{140}Ce is a probe nuclei specific to study the magnetic hyperfine field (B_{hf}) (due to its low electric quadrupole moment only dipole magnetic interactions are observed), it can be determined with high precision. In addition, their structural and morphology characteristic were checked by X-ray diffractions (XRD) and Transmission Electron Microscopy (TEM) respectively.

II. EXPERIMENTAL PROCEDURE

A. Sample preparation

Samples were synthesized by Sol-Gel rout from the starting materials La_2O_3 , $\text{Ba}(\text{NO}_3)_2$, and Mn powders with minimum purity of 99.95%. All starting materials were dissolved in nitric acid solution under magnetic stirring and heating (about 50°C). After mixed the starting materials and added ethylene glycol and citric acid. The solution was in magnetic stirring and heating (about 120°C) by some hours. The gel resulting was calcined in 550°C by 12 hours. Finally, the powder resulting was heated at 1100°C for 48 hours. Annealing and calcination was carried out under air atmosphere.

B. Structural and morphological characterization

The structure and morphology of samples were then characterized by XRD and TEM. The XRD results, displayed in Fig. 1, show that samples of perovskite oxides present a cubic structure with the $Pm\text{-}3m$ space group corresponding to the $\text{La}_{0.5}\text{Ba}_{0.5}\text{MnO}_3$ phase, which occurs due to an oxygen deficiency. When there is no oxygen deficiency, perovskite oxides present the regular $\text{LaBaMn}_2\text{O}_6$. Diffraction pattern of the sample can be seen in Fig. 1 along with the Rietveld fit from which the lattice parameter obtained is displayed in Table I.

The XRD measurements were performed at LCT-laboratory at Polytechnic Institute of University of São Paulo (USP). The data were analyzed by the Rietveld method with software Rietica.⁹ Table I shows the results of Rietveld refinement and a comparison of the

TABLE I. Data of experimental and theoretical lattice parameter and Rp for $\text{La}_{0.5}\text{Ba}_{0.5}\text{MnO}_3$ compound.

Sample	Exp. lattice parameter (Å)	Theo. lattice parameter (Å)	Rp
$\text{La}_{0.5}\text{Ba}_{0.5}\text{MnO}_3$	3.9919(47)	4.0003(2) ⁸	9.80

experimental lattice parameter with the theoretical one. The quality of refinement can be verified by Rp (profile R-factor) parameter that is a numerical statistical indicator. The analysis showed only one phase but the XRD pattern presents few very small peaks that couldn't be identified.

TEM micrographs are showed in Figure 2-A it's suggested the formation of nanorod-like particles form and it can see a good distribution in all sample. The accurate inspections in one of these nanorod-like particles by the TEM are displayed in the Figure 2B. The resolution of image revealed only one mono-domain region with homogenous crystallographic planes but in a layer or around 1-2 nm near the surface it is possible to observe irregularities in the plane lines. This result supports the stable phase, the separation on crystalline plane is the average interfringe distance of nanocrystals was measured to be ~ 0.41 nm this value is in agree with lattice parameter obtained by Rietveld analysis. Both results, XRD pattern and TEM images, suggest a stable crystal lattice structure of $\text{La}_{0.5}\text{Ba}_{0.5}\text{MnO}_3$.

C. Local study by perturbed angular correlation (PAC) spectroscopy

PAC technique is based on the observation of hyperfine interaction nuclear moments with extra-nuclear magnetic field or electric gradient. More detailed can be found elsewhere.^{10,11} This method uses a radioactive probe nuclei for the measurements and, in this work, we used ^{140}La (^{140}Ce) and $^{111\text{m}}\text{Cd}$ (^{111}Cd) as probe nuclei replacing La and Mn lattice position in $\text{La}_{0.5}\text{Ba}_{0.5}\text{MnO}_3$, respectively. Results from PAC experiments are the spin-rotation spectra $R(t) = A_{22} \sum_i f_i G_{22}^i(t)$, where A_{22} is the angular correlation coefficient, fitted by a model that taken into account the fractional site population (f) of probe nuclei and their respective perturbation function $G_{22}(t)$. A_{22} are -0.092 and +0.175 for ^{140}La (^{140}Ce) and $^{111\text{m}}\text{Cd}$ (^{111}Cd),¹² respectively. Because A_{22} is negative, the

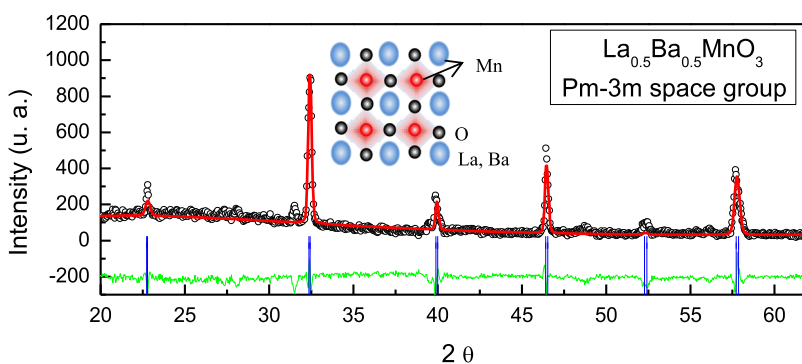


FIG. 1. XRD patterns for $\text{La}_{0.5}\text{Ba}_{0.5}\text{MnO}_3$ compound. Black circles are the experimental data, red line is the Rietveld fit, green line is the difference between experimental data and the fit, and horizontal blue lines indicate the theoretical peaks positions. A bi-dimensional crystal structure representation of the cubic $Pm\text{-}3m$ single perovskite structure is also displayed.

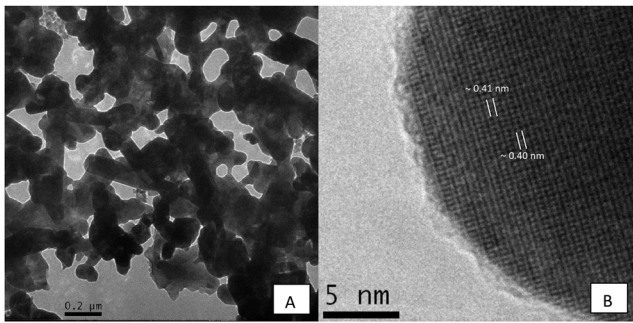


FIG. 2. TEM image after calcination at 550°C. The particles are shown in dark contrast and the white regions are spaces between particles. A) With a scale bar of 0.2 μm the image shows the formation of nanorod-like particles. B) With a scale bar of 5 nm and the image displaying one selected nanoparticle the atomic plane lines can be seen. The atomic plane lines are regular in the inner part of the particles but are non-regular in a layer near the surface.

spin-rotation spectra for $^{140}\text{La}(^{140}\text{Ce})$ are displayed as $-R(t)$ with the y axis inverted. For magnetic hyperfine interactions, $G_{22}(t) = 0.2 + 0.4 \sum_{n=1,2} \cos(n\omega_L t)$ and its measurement allows the determination of the Larmor frequency $\omega_L = \mu_N g B_{\text{hf}} / \hbar$, where μ_N is the nuclear magneton and g is the nuclear g -factor, and the calculation of the magnetic hyperfine field B_{hf} . The perturbation function for electric quadrupole interactions is given by $G_{22}(t) = S_{20} + \sum_{n=1,2,3} S_{2n}(\eta) \cos(g_n(\eta) \nu_Q t)$, where the quadrupole frequency $\nu_Q = eQV_{zz}/h$ and the asymmetry parameter $\eta = (V_{xx} - V_{yy})/V_{zz}$, can be experimentally determined allowing the calculation of the components V_{kk} , $k = x, y, z$ of the electric field gradient tensor.

The experimental data were acquired using PAC spectrometers with six and four detectors arrangement. The experimental data were fitted by using a model that takes into account the only magnetic dipole interactions for the case of measurements with

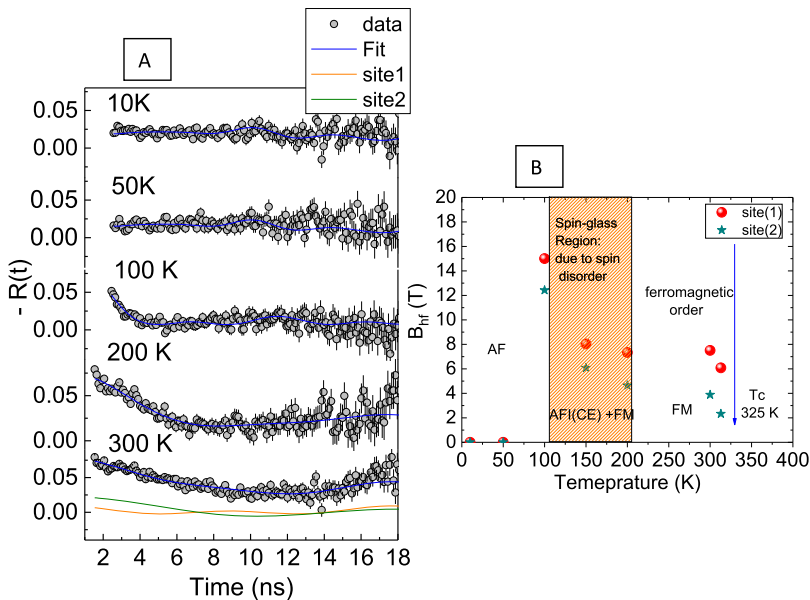


FIG. 3. (A) PAC spectra for ^{140}Ce probe nuclei. Site 1 and site 2 are represented as green and red solid lines, respectively; constituting the two components of the spectrum measured at 300 K. (B) Magnetic Hyperfine Field (B_{hf}) as function of temperature to site 1 (defective) and site 2 (regular). This result shown well defined region AF (antiferromagnetic order), AFI(CE) phase coexisting with the FM phase and Ferromagnetic phase (FM) above 200K with Temperature Transition $T_C \sim 325\text{K}$.

$^{140}\text{La}(^{140}\text{Ce})$ probe nuclei and for the case of $^{111\text{m}}\text{Cd}(^{111}\text{Cd})$, a combined electric quadrupole plus magnetic dipole interaction has been used.

III. RESULTS AND DISCUSSIONS

$^{140}\text{La} \rightarrow ^{140}\text{Ce}$ probes: In order to activated ^{140}La probe nuclei (present as natural Lanthanum isotope ^{139}La), after synthesis samples were irradiated with neutrons in the pneumatic station of the IEA-R1 nuclear research reactor of IPEN for 3 minutes with a thermal neutrons flux of about $6 \times 10^{12} \text{ n cm}^{-2} \text{ s}^{-1}$. In order to verify the activation, gamma emission measurements of the samples were performed using a HP(Ge) detector (Model GC 3020) coupled to a digital spectrum analyzer (DSA-1000), both from Canberra. Samples were measured after 1, 18, 24 and 48 h of decay times and counting time was of 600 seconds. This method could be used because natural La is present in samples and the location of the probe nuclei for PAC measurements in the crystalline structure is unambiguously determined.

The gamma energies of 328.8 keV and 487.0 keV of ^{140}La (used in the PAC spectroscopy) could be identified. Besides this, gamma-rays peaks of ^{56}Mn (E_γ of 847.3 and 1812.9 keV and $t_{1/2}$ of 2.57 h) and ^{139}Ba (E_γ of 166.04 keV and $t_{1/2}$ of 84.63 min) were identified with much higher intensities. But after 48 h of decay time show only the gamma peaks of ^{140}La , during this period the sample was annealed at 800 °C. Therefore, PAC measurements with $^{140}\text{La}(^{140}\text{Ce})$ probe nuclei were carried out 10 K to 300 K and the spin-rotation $R(t)$ spectra can be seen in the Figure 3–B. The analyses were made using two dipolar magnetic sites.

Although the measurements were performed with ^{140}Ce probe nuclei, it is expected that these probes be at the unique La positions in the crystalline structure because ^{140}Ce nuclei result from the beta-decay of ^{140}La . However, our results show that ^{140}Ce occupy two site fractions with different Magnetic Hyperfine Field (B_{hf}). The major fraction (site 2 in Fig. 3) with lower B_{hf} is ascribed probes at regular

La sites, whereas the minor fraction (site 1 in Fig. 3) with higher B_{hf} is assigned to probes at defective La sites probably with Oxygen vacancies in their nearest neighbor.

Figure 3-B shows the B_{hf} at La sites measured with ^{140}Ce as function of temperature. For both site fractions of probe nuclei, we can observe the ferromagnetic transition around 325 K followed by an antiferromagnetic transition below 200 K as showed in previous paper.⁷ Below this transition temperature, AFI(CE) phase coexists with the FM phase. However, below around 100 K ω_L results show that only antiferromagnetic interactions are predominant since at La sites the transferred field from Mn ions cancels due to the spin structure (see Fig. 3a) formed by these magnetic ions. Therefore, no modulation in $R(t)$ spectra was observed below 100 K, this occurrence can be attributed to predominant antiferromagnetic transition characteristic of this double perovskite. In antiferromagnetic phase, the transferred field from the nearest Mn neighbors cancels at La site, then this is the reason that the frequency was drove to vanish. Second, the amplitude of the $R(t)$ spectra (anisotropy) in antiferromagnetic region are very low when compared to those for the ferromagnetic region, this low anisotropy can be attributed to a spin glass behavior due to spin disorder. Spin glass behavior is in accordance with previous studies in $\text{Y}_{0.5}\text{Ba}_{0.5}\text{MnO}_3$ below 50 K.¹³

$^{111}\text{mCd} \rightarrow ^{111}\text{Cd}$ probes: ^{111}mCd ($t_{1/2} = 49$ min) nuclei were implanted into pellet samples of $\text{La}_{0.5}\text{Ba}_{0.5}\text{MnO}_3$ at the on-line isotope separator ISOLDE at CERN with implantation energies of 60 keV and a dose of 10^{12} cm^{-2} for each implantation. In order to remove the implantation damage, samples were annealed in air with different thermal history in order to obtained good resolution of the spin rotation spectra $R(t)$. Resulting PAC spectra are displayed in Fig. 4, where, at the top, the first measurement taken after annealing at 850 °C following the implantation can be seen. This $R(t)$ spectrum presents a broad frequency distribution (characterized by a strong damping of amplitude after few ns), This damping suggests that probably probe nuclei are trapped at the interstitial positions and or strong disorder due implantation damage is present in the sample. On the other hand, with annealing at 1000°C (see Fig. 4, middle and bottom spectra) we could observe a good modulation of $R(t)$ spectra with very low damping. These characteristics indicate that probe nuclei are at substitutional sites and have replaced cationic atoms in the crystalline lattice of the $\text{La}_{0.5}\text{Ba}_{0.5}\text{MnO}_3$.

The fits of spectra for $^{111}\text{mCd}(^{111}\text{Cd})$ were performed using a model in which a combined electric quadrupole plus magnetic dipole interaction are considered. Due to the similarity of the ionic radius values of Cd and La, we suppose that ^{111}mCd probes replace the position of La atoms.¹⁴ In addition to support this assumption is the fact that B_{hf} vanishes below 100 K due to the spin cancel at La positions in the AF phase.⁷ Results of the fit of spectrum measured at room temperature (RT) after annealing at 1000 °C show that probe nuclei occupy a single site fraction characterized by a quadrupole frequency $\nu_Q = 84.2(5)$ MHz, asymmetry parameter $\eta = 0.16(2)$ and magnetic frequency $\nu_M = 0.64(1)$ MHz ($B_{hf} \approx 0.03$ T) and angle between directions of both interactions $\beta = 90^\circ$. Measurements at 77 K yielded quite similar electric quadrupole parameters: $\nu_Q = 81.6(6)$ MHz and $\eta = 0.16(2)$, whereas a null magnetic interaction has been observed.

The values of B_{hf} at regular La sites measured with ^{140}Ce increases when temperature decreases below around 320 K and seem to follow a standard magnetization curve. In the FM region B_{hf}

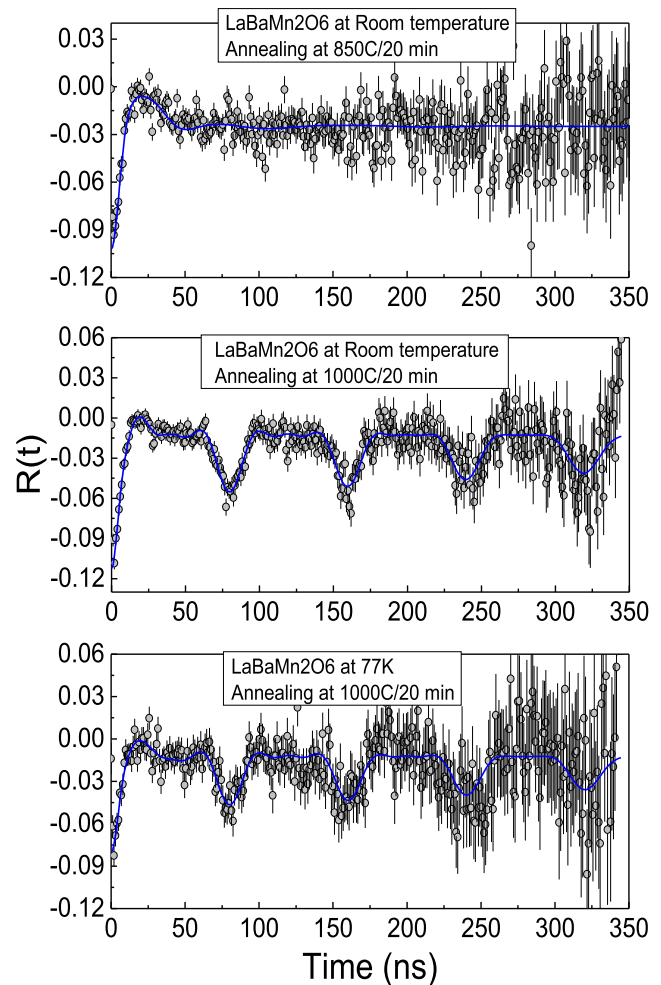


FIG. 4. Spin-rotation spectra measured with ^{111}mCd probe nuclei implanted into samples at ISOLDE/CERN and measured at 295 K and 77 K.

reaches 5.7 T, which is close to the value of 5.2 T estimated for the FM phase in $\text{LaBaMn}_2\text{O}_6$ when measured with NMR using ^{139}La as probe nuclei.⁷ Below around 150 K, B_{hf} increases sharply most probably due to the polarization of the 4f electron in Ce.¹⁴ The small value of B_{hf} measured with ^{111}Cd at RT indicates a super exchange mechanism via oxygen orbitals between Mn magnetic ions and La ions which is weaker when the bond angle is near 90° . B_{hf} is null for both probe nuclei below 100 K indicating a pure AF interaction and ruling out the possibility of the co-existence of FM plus AF interactions.

IV. CONCLUSION

Experimental data from hyperfine interactions measurements in $\text{La}_{0.5}\text{Ba}_{0.5}\text{O}_3$ using different probe nuclei constitute a very interesting tool to characterized chemical and physical properties in complex oxides such as double perovskites. In the present work, PAC measurements using $^{140}\text{La}(^{140}\text{Ce})$ showed that only magnetic dipole

interactions are detected with good precision allowing the determination of magnetic transition phases characterized by $T_C = 325$ K (PM to FM) and $T = 200$ K (FM to AF(CE)+FM) and $T_N \sim 100$ K (AFM). On the other hand, the amplitude of $R(t)$ spectra was a sensitive parameter to detected order or disorder in magnetic phases of this sample. The magnetic disorder showed in these samples are due to spin glass behavior, which is characteristic of double perovskites. Furthermore, ^{111}Cd present a strong evidence that the sample doesn't have a structural transition in the range of 295 K to 77 K but, in order to confirm this supposition, measurements at different temperatures within this range are necessary. The evidence of no structural transition reinforces the conclusions obtained from measurements with ^{140}Ce about magnetic transitions and the spin glass behavior due to only a spin disorder region and not due to structural transition phase.

ACKNOWLEDGMENTS

We thank the financial support received from the Federal Ministry of Education and Research (BMBF) through grant 05K16PGA and the Foundation for Science and Technology FCT via grants CERN-FIS-NUC-0004-2015 and CERN-FIS-PAR-0005-2017. We also acknowledge the support from the European Union's Horizon 2020 Framework research and innovation programme under grant agreement no. 654002 (ENSAR2). Finally, we would like to thank the Conselho Nacional de Pesquisa e Desenvolvimento Científico (CNPq), grant no. 304627/2017-8 and Fundação de Amparo a Pesquisa do Estado de São Paulo (FAPESP) by financial support under grant no. 2017/50332-0.

REFERENCES

- ¹A. K. Kundu and B. Raveau, *Nova Publishers* **1**, 213–250 (2010).
- ²L. Er-Rakho, C. Michel, P. Lacorre, and B. Raveau, *J. Solid State Chem.* **73**, 531 (1988).
- ³Y. Kawasaki, T. Minami, Y. Kishimoto, T. Ohno, K. H. Satoh, A. Koda, R. Kadono, T. Nakajima, and Y. Ueda, *J. Phys.: Conference Series* **391**, 012096 (2012).
- ⁴S. Bao, C. Ma, G. Chen, X. Xu, E. Enriquez, C. Chen, Y. Zhang *et al.*, *Scientific Reports* **4**, 4726 (2014).
- ⁵Y. Ueda and T. Nakajima, *J. Phys.:Condens. Matter* **16**, S573 (2004).
- ⁶Y. Kawasaki, T. Minami, Y. Kishimoto, T. Ohno, K. H. Satoh, A. K. R. Kadono, T. Nakajima, and Y. Ueda, *Journal of Physics: Conference Series* **391**, 012096 (2012).
- ⁷Y. Kawasaki, T. Minami, Y. Kishimoto, T. Ohno, K. H. Satoh, A. K. R. Kadono, T. Nakajima, and Y. Ueda, *Phys. Rev. Lett.* **96**, 037202 (2006).
- ⁸H. J. Kitchen, I. Saratovsky, and M. A. Haywar, *Dalton Transactions* **39**, 6098–6105 (2010).
- ⁹C. J. Howard and B. A. Hunter, *A Computer Program for Rietveld Analysis of X-Ray and Neutron Powder Diffraction Patterns—RIETICA* (Australian Nuclear Science and Technology Organization Lucas Heights Research Laboratories, Australia, 1997).
- ¹⁰A. W. Carbonari, R. N. Saxena, W. Pendl, Jr., J. Mestnik-Filho, R. N. Attili, M. Olzon-Dionysio, and S. D. Souza, *J. Magn. Magn. Mater.* **163**, 313 (1996).
- ¹¹R. Dogra, A. C. Junqueira, R. N. Saxena, A. W. Carbonari, J. Mestnik-Filho, and M. Morales, *Phys. Rev. B* **63**, 224104 (2001).
- ¹²H. H. Rinneberg, *Atomic Energy Reviews* **17**, 477–595 (1979).
- ¹³W. Sato, S. Komatsuda, A. Osa, T. K. Sato, and Y. Ohkubo, *Hyperf. Interact.* **237**, 113 (2016).
- ¹⁴A. W. Carbonari, J. Mestnik-Filho, R. N. Saxena, and M. V. Lalic, *Phys. Rev. B.* **69**, 144425–144427 (2004).